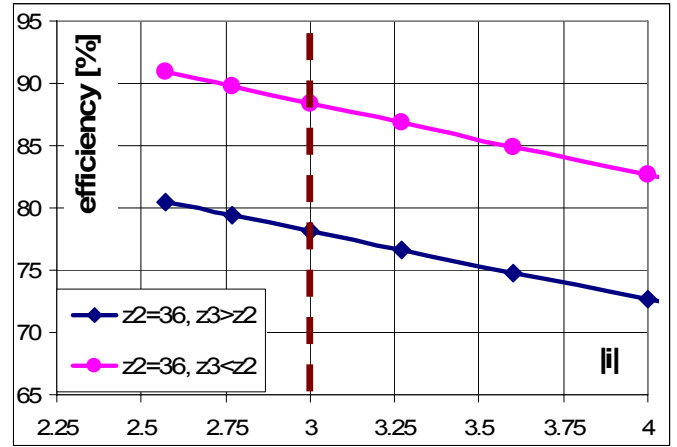
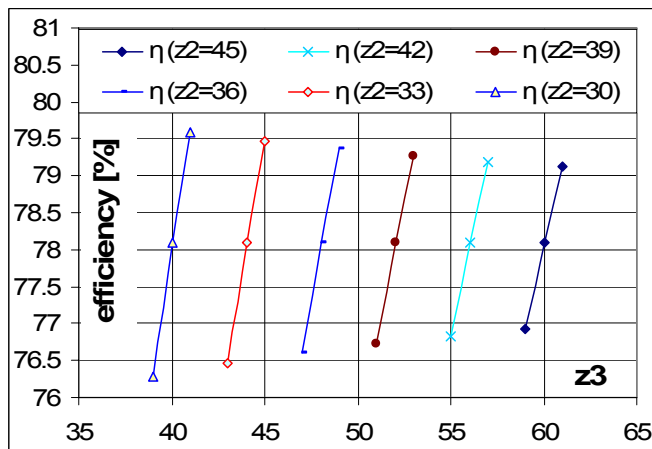


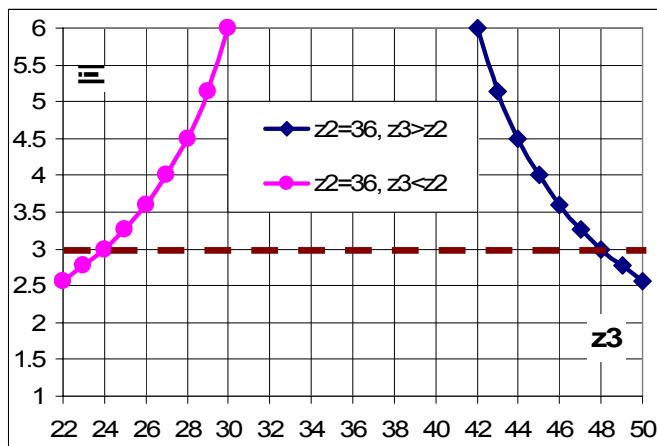
a)



d)



b)



c)

Fig. 3. Numerical simulations for: d) the efficiency in the cases \$z_3 < z_2\$ and \$z_3 > z_2\$ for \$z_2=36\$.

The angular speeds and accelerations transmission functions (rel. 5) can be established based on relation (2), while the moments transmission function (rel. 6) based on relation (3), [4, 7]:

$$i_{1H}^3 = \frac{\omega_{13}}{\omega_{H3}} \Rightarrow \omega_{H3} = \frac{\omega_{13}}{i_{1H}^3} = 3 \cdot \omega_{13}; \quad \varepsilon_{H3} = \frac{\varepsilon_{13}}{i_{1H}^3} = 3 \cdot \varepsilon_{13} \quad (5)$$

$$\eta = \eta_{1H}^3 = \frac{-\omega_{H3} T_H}{\omega_{13} T_1} \Rightarrow T_H = T_1 \cdot i_{1H}^3 \cdot \eta_{1H}^3; \quad (6)$$

in the case of neglecting friction, the moments transmission function is given by the following relation:

$$T_H = T_1 \cdot i_{1H}^3 = \frac{T_1}{3} = 0.3333T_1$$

while in the case of considering friction, the function becomes:

$$T_H = T_1 \cdot i_{1H}^3 \cdot \eta_{1H}^3 = T_1 \cdot 0.3333 \cdot 0.781 = 0.2603T_1$$

3 Premises for Dynamic Modeling

The speed increaser dynamic modeling relies on the following premises:

- the dynamic model used in the paper is a simplified one, but with acceptable differences versus the real dynamic response [2, 6]; the considered accuracy is sufficient for this paper objective. The simplification consists in the following presumptions:

- 1) it is considered that the correlations generated by the planetary unit among the torques \$T_1\$, \$T_H\$ and \$T_3\$ (see Fig. 4,a) can be modeled in static conditions;

Fig. 3. Numerical simulations for different combinations of teeth numbers of a) the multiplication ratio (multiplied 10 times), b) the efficiency, c) the multiplication ratio in the cases \$z_3 < z_2\$ and \$z_3 > z_2\$, for \$z_2=36\$ teeth.

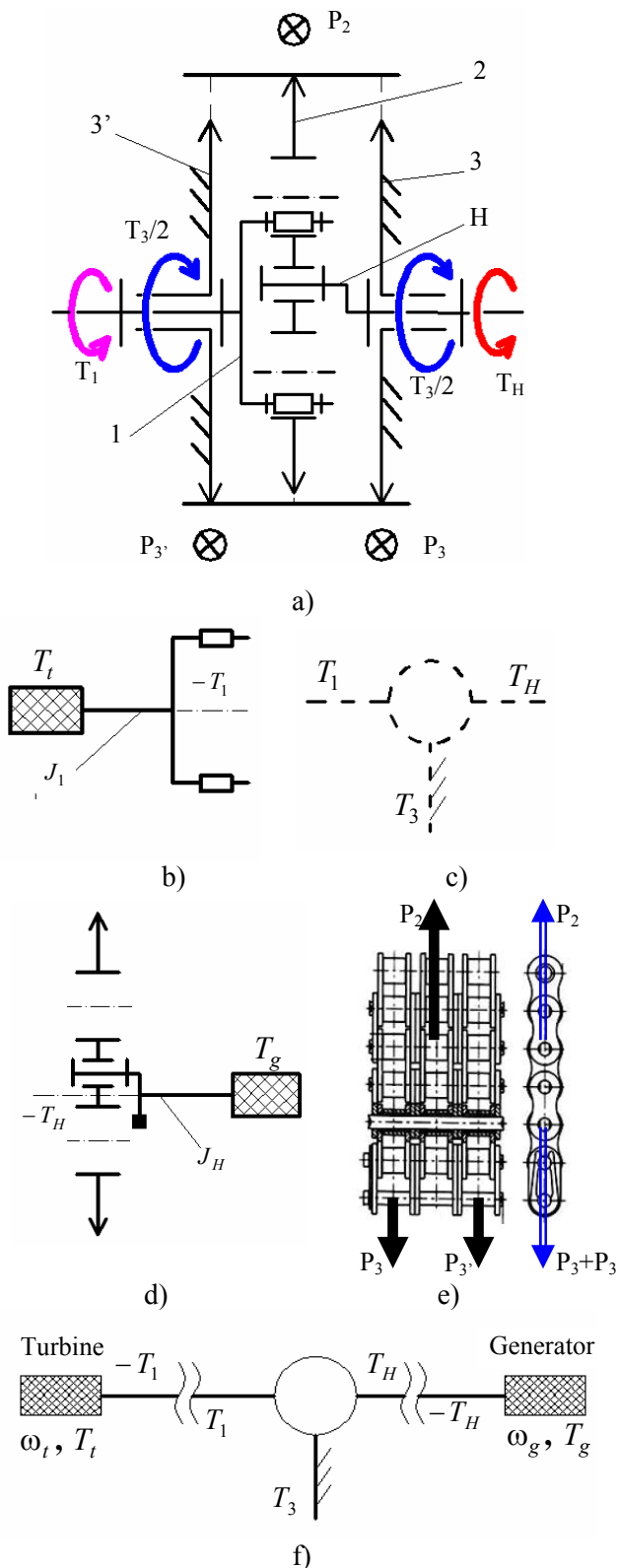


Fig. 4. The scheme of the chain planetary increaser: a) the external torques of the planetary unit and the chain forces, b) the dynamic scheme for the input element, c) the block diagram of the planetary speed increaser, d) the dynamic scheme for the output element, e) the chain forces' configuration, f) the block scheme of the considered machine (water turbine – speed increaser - electric generator).

2) the inertial moments of the satellite mass and, partially, of the chain are included in the mechanical inertia momentum of the output shaft (see Fig. 4,d);
 3) the inertial effects of the central element 1 and, partially, of the chain are included in the mechanical inertia momentum of the input shaft (Fig. 4,b);
 thus, the inertial effects due to the satellite gear rotation are neglected (its mass being considered in the axial inertial moment of the afferent carrier shaft), while the inertial effects of the mobile central elements are considered integrated into the shafts that materialize the external links of the planetary gears; under this premise, the static correlations between the external torques of each planetary gear are valid (Fig. 4,a), while the dynamic correlations interfere only for the shafts that materialize the planetary gears external links. The mechanical inertia momentums of the two shafts (see Fig. 4) are:

$$J_1 = 0.035 ; J_H = 0.02 [Kgm^2] \tag{7}$$

- the rubbing effect is considered by means of the efficiency η ;
- the turbine and generator are characterized by a power – speed characteristic and an efficiency – speed characteristic; in order to obtain the mechanical characteristics, the Turgo turbine and the generator were tested for different speeds on experimental stands (see Fig. 5); the results allow the establishment of the turbine and generator moment – speed characteristics, and, also, highlight the fact that the turbine efficiency is higher for lower speeds while the generator performances are better for higher speeds. The mechanical characteristics of the turbine and of the generator on their own shaft, used in the dynamic numerical simulations, have the following expressions (Fig. 6 and 7):



Fig. 5. The generator parameters identification on experimental stand

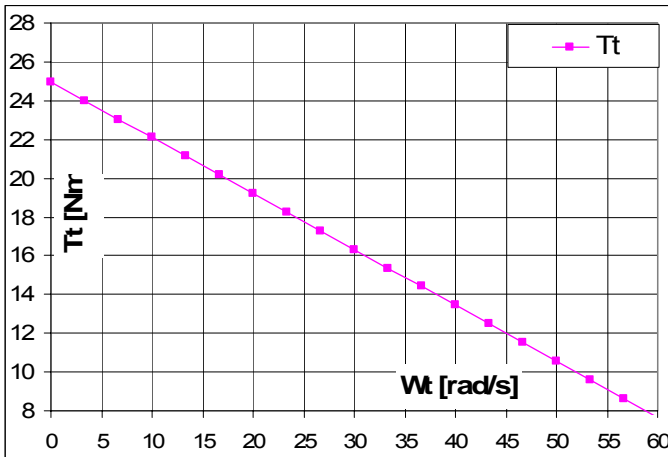


Fig. 6. The turbine mechanical characteristic

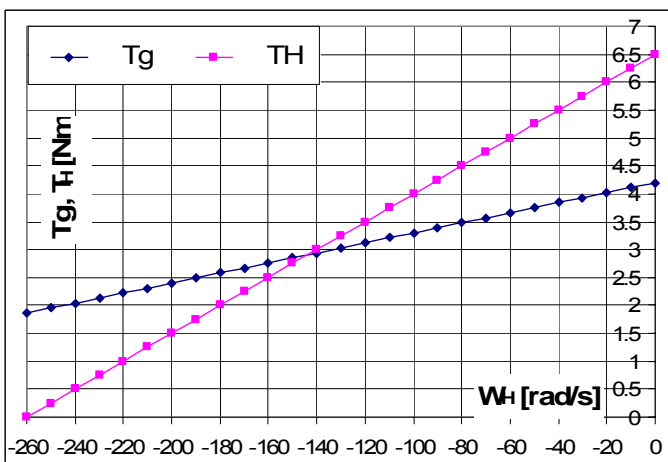


Fig. 7. The generator mechanical characteristic (Tg), the turbine mechanical characteristic reduced on the output shaft (-TH) and the stationary working point

$$T_t = -0.2881 \cdot \omega_b + 24.967 \text{ [Nm]} \tag{8}$$

$$T_g = -0.009 \cdot \omega_g + 4.2 \text{ [Nm]} ;$$

- In order to establish the working point, the turbine mechanical characteristic is reduced to the speed increaser output shaft as $T_H = T_t(\omega_H)$; then, the two characteristics, of the turbine and generator are superposed (see Fig. 7).
- in the numerical simulations, the following values for the kinematical and dynamic parameters are considered:
 - the satellite and sun gears teeth numbers are $z_2 = 36, z_3 = 48$, for a module $m = 3 \text{ mm}$,
 - the efficiencies of the pin coupling and chain transmission are $\eta_{12} = 0.995, \eta_{23} = 0.95$ [1, 4].

4 The Dynamic Model

In the dynamic modeling, the main objectives are to find the machine working point in stationary regime and the transmission functions for the angular speeds, accelerations and moments, relative to time:

$$\omega_t = \omega_t(t), \omega_{13} = \omega_{13}(t), \omega_{H3} = \omega_{H3}(t), \omega_g = \omega_g(t),$$

$$\varepsilon_t = \varepsilon_t(t), \varepsilon_{13} = \varepsilon_{13}(t), \varepsilon_{H3} = \varepsilon_{H3}(t), \varepsilon_g = \varepsilon_g(t), \tag{9}$$

$$T_t = T_t(t), T_1 = T_1(t), T_H = T_H(t), T_g = T_g(t).$$

The validation of the dynamic model will be made by checking the concordance between the values of the speed and moment in stationary regime given by the dynamic model and the values of speed and moment corresponding to the working point.

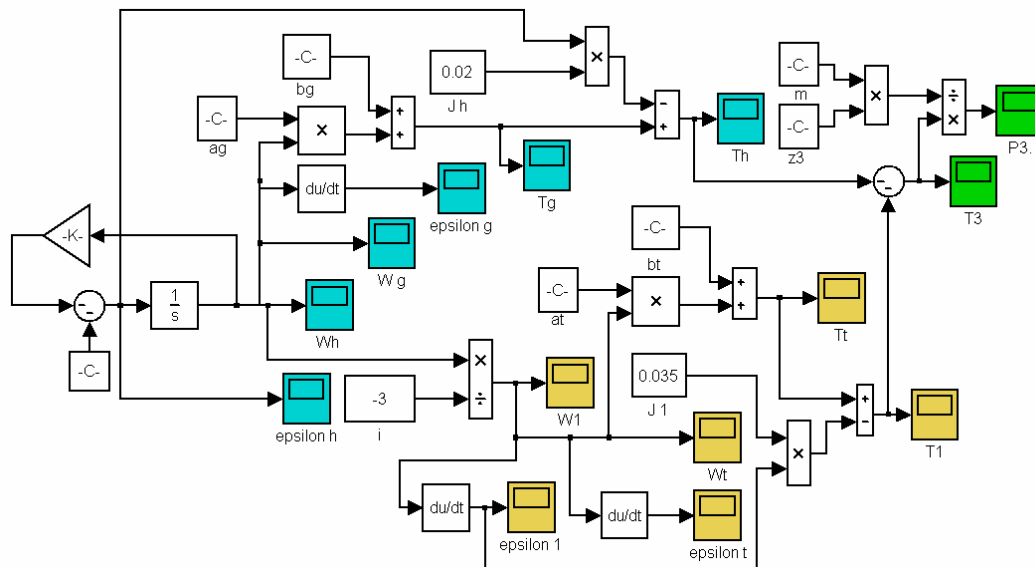


Fig. 8. The Simulink scheme that models the motion equation of the turbine-speed increaser-generator assembly

The working point in the stationary regime is given by the intersection of the turbine and generator characteristics (see Fig. 7) and is characterized by a speed $\omega_H = -143.6659$ [rad/s] and a moment $T_H = 2.9$ [Nm].

The dynamic modeling is made by means of Fig. 4, b,c, d, e and f, for the following cases:

- The motion equation is modeled by neglecting friction, and
- The motion equation is modeled by considering friction.

4.1 Case I, friction is neglected

In this case the Lagrange method is being used [7]:

$$\frac{d}{dt} \left(\frac{\partial E_c}{\partial \omega} \right) - \left(\frac{\partial E_c}{\partial \varphi} \right) = Q \quad (10)$$

According to Fig. 4, the kinetic energy E_c and generalized force Q have the following forms, in which $d\varphi/dt = d\varphi_H/dt = \omega_H$ represents the independent speed:

$$\begin{aligned} E_c &\cong \frac{1}{2} (J_1 \cdot \omega_1^2 + J_H \cdot \omega_H^2); \\ Q \cdot \omega_H &= T_t \cdot \omega_1 + T_g \cdot \omega_H \Rightarrow \\ Q &= T_t \cdot i_{1H}^3 + T_g \end{aligned} \quad (11)$$

in which J_1 , represents the mechanical inertia momentum of the input element 1, respectively J_H , for the output element H (see Fig. 4).

Deriving E_c relative to time, it is obtained:

$$\begin{aligned} \frac{\partial E_c}{\partial \omega_H} &= \omega_1 J_1 \cdot \frac{\partial \omega_1}{\partial \omega_H} + \omega_H J_H; \\ \frac{d}{dt} \left(\frac{\partial E_c}{\partial \omega_H} \right) &= \varepsilon_1 (1 - i_0) J_1 + \varepsilon_H J_H; \\ \frac{d}{dt} \left(\frac{\partial E_c}{\partial \varphi} \right) &= 0 \end{aligned} \quad (12)$$

From relations (11) and (12) it results:

$$\begin{aligned} \varepsilon_1 (1 - i_0) J_1 + \varepsilon_H J_H &= T_t \cdot i_{1H}^3 + T_g \\ \varepsilon_1 (1 - i_0) J_1 + \varepsilon_H J_H &= T_t (1 - i_0) + T_g \\ \varepsilon_1 &= i_{14}^3 \cdot \varepsilon_H = (1 - i_0) \varepsilon_H \\ \varepsilon_H [J_1 (1 - i_0)^2 + J_H] &= T_t (1 - i_0) + T_g \\ T_t &= a_t \omega_t + b_t, \quad T_g = a_g \omega_g + b_g \\ \varepsilon_H [J_1 (1 - i_0)^2 + J_H] &= (a_t \omega_t + b_t) (1 - i_0) + a_g \omega_g + b_g \\ \varepsilon_H [J_H + J_1 (1 - i_0)^2] - a_t \omega_t (1 - i_0) + & \\ + b_t (1 - i_0) - a_g \omega_g - b_g &= 0 \end{aligned} \quad (13)$$

For $\omega_t = \omega_1 = (1 - i_0) \omega_H$ and $\omega_t = \omega_H$, the previous relation becomes:

$$\varepsilon_H [J_H + J_1 (1 - i_0)^2] - a_t \omega_t (1 - i_0)^2 + b_t (1 - i_0) - a_g \omega_H - b_g = 0$$

By replacing the known parameters into relation (13), the dynamic equation when neglecting friction outcomes:

$$\varepsilon_H [J_H + J_1 (1 - i_0)^2] - \omega_H [a_t (1 - i_0)^2 + a_g] - b_t (1 - i_0) - b_g = 0 \quad (14)$$

where $a_t = -0.28818$ [Nms]; $b_t = 24.967$ [Nm];

$a_g = 0.009$ [Nms]; $b_g = 4.2$ [Nm];

$J_H = 0.02$ [Kgm²]; $J_1 = 0.035$ [Kgm²]

and $1 - i_0 = 0.3333$.

After numerical replacements, the following motion equation results:

$$\varepsilon_H \cdot 0.023889 + \omega_H \cdot 0.02302 + 4.12225 = 0 \quad (15)$$

4.1 Case II, friction is considered

In this case, according to Fig. 4,b, c, d and e, the following system of equations can be written using the Newton-Euler method:

$$\begin{aligned} T_1 + T_H + T_3 &= 0; \\ T_1 \cdot i_{1H}^3 \cdot \eta_{1H}^3 + T_H &= 0; \\ T_1 \cdot i_0 \cdot \eta_0 + T_3 &= 0; \\ J_1 \varepsilon_1 &= T_m - T_1; \\ J_H \varepsilon_H &= T_b - T_H. \end{aligned} \quad (16)$$

The following relation is obtained through successive replacements:

$$\varepsilon_H [J_H + J_1 (1 - i_0)^2 \cdot \eta_{1H}^3] - T_t (1 - i_0) \eta_{1H}^3 - T_g = 0$$

By taking into account friction, the equation used for modeling the machine dynamic system is obtained:

$$\varepsilon_H [J_H + J_1 (1 - i_0)^2 \cdot \eta_{1H}^3] - \omega_H [a_t (1 - i_0)^2 \eta_{1H}^3 + a_g] - b_t (1 - i_0) \eta_{1H}^3 - b_g = 0. \quad (17)$$

After numerical replacements, the following motion equation results:

$$\varepsilon_H \cdot 0.023037 + \omega_H \cdot 0.01601 + 2.299677 = 0 \quad (18)$$

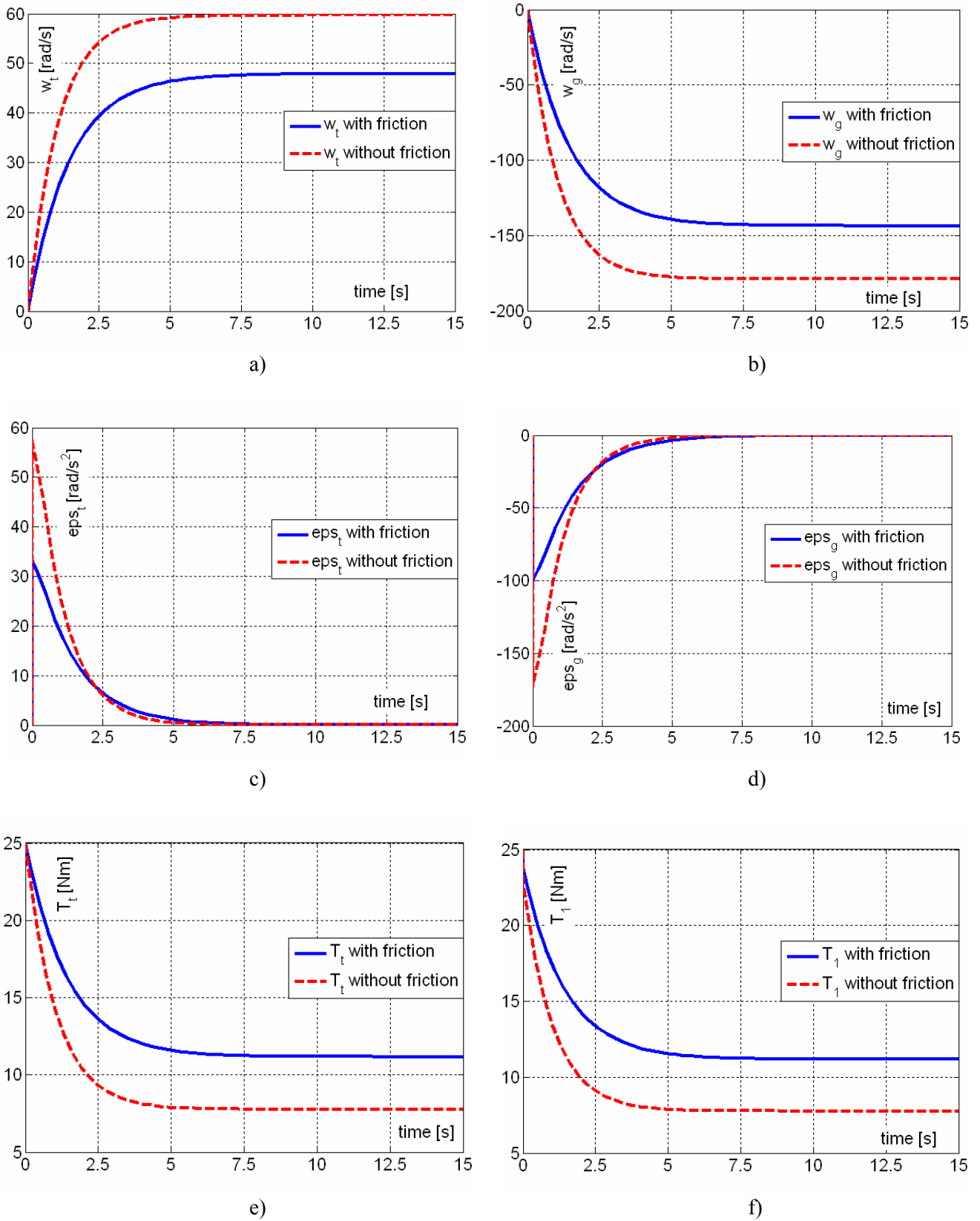


Fig. 9. Dynamic response of the assembly: turbine angular speed (a), generator angular speed (b), turbine angular acceleration (c), generator angular acceleration (d), turbine moment (e), input moment (f)

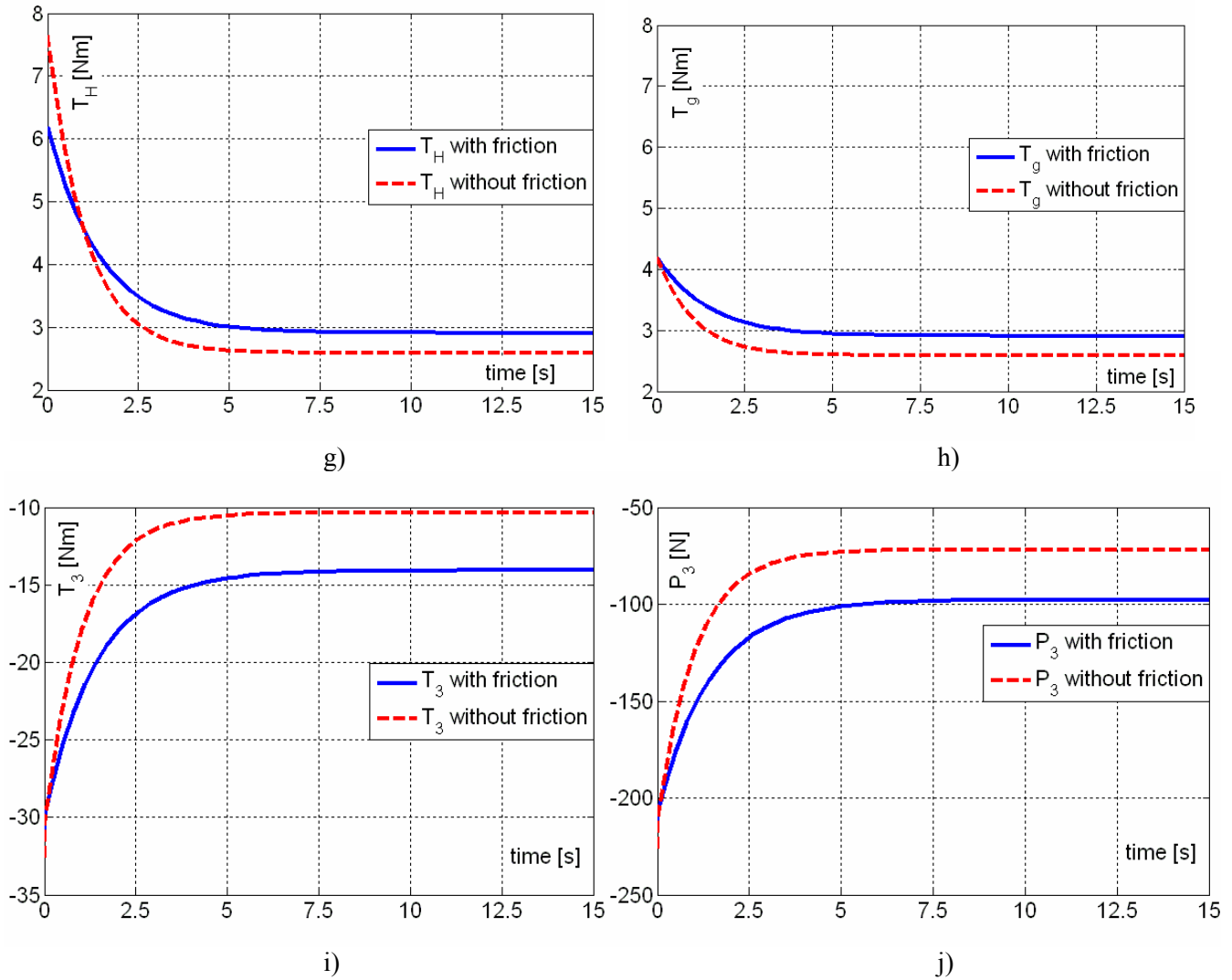


Fig. 9. Dynamic response of the assembly: output moment (g), generator moment (h), moment on the sun gear 3 (i), and force on chain (j).

Relation (18) represents the Turgo assembly motion equation in the case of considering friction. It can be easily observed that relation (15) is a particular case of relation (17).

5 Numerical Simulations

The values of the output and input angular speeds in stationary regime ($\varepsilon_H = 0$) are obtained from relations (15) and (18):

- when friction is neglected:
 $\omega_H = -179.078$; $\omega_1 = 59.69191$, [rad/s]
- when friction is considered:
 $\omega_H = -143.6659$; $\omega_1 = 47.88816$. [rad/s]

The Simulink scheme that models the motion equation of the turbine - planetary speed increaser – generator

assembly is presented in Fig. 8. The machine dynamic response, which consists of the speeds, accelerations and moments as functions of time, for the turbine, speed increaser and electric generator are depicted in the Fig. 9. The variations of the increaser input and output speeds and accelerations are not represented as they coincide to the speeds and accelerations of the turbine and generator, respectively. The forces that act on the chain, P_2 , P_3 and P_3' (Fig. 4,e) are given by the following relation, which is valid when neglecting the chain inertia:

$$P_3 \cong P_3' = \frac{T_3/2}{r_3} = \frac{T_3}{d_3} = \frac{T_3}{m_3 \cdot z_3};$$

where $m_3 = m = 3$ mm is the gears' module. For the model validation, the working point values are compared to the simulation results; it can be observed that the values of speed and moment in the stationary

preparation and publishing of this paper were possible with the financial support of this research project.

8 CORRESPONDING ADDRESS

Professor dr. eng. Codruta Jaliu
Transilvania University of Brasov,
Product Design and Robotics Department
Eroilor 29, 500036 Brasov, Romania
Phone/Fax: +40 268 472496,
E-mail: cjaliu@unitbv.ro

References:

- [1] American Chain Association, *Standard Handbook of Chains: Chains for Power Transmission and Material Handling*, 2nd Edition, Dekker Mechanical Engineering, 2005.
- [2] Chereches, T., Sava, AC. *Some aspects regarding the using of the dynamics arrays in the numerical simulation of the hydraulic and pneumatic devices*, Proc. Of the 6th IASME/WSEAS International Conference on Fluid Mechanics and Aerodynamics FMA'08, pp. 264-268, Aug. 20-22, 2008, Rhodes, Greece.
- [3] Cristea, L. *The Improvement of Performances in Automatic Dimensional Inspection for Bearing Production, an Important Way to Quality Assurance in Mechanical Engineering*, Proceedings of the 8th international conference on instrumentation, measurement, circuits and systems (IMCAS 09). Hangzhou, China: WSEAS, 2009. ISSN 1790-5117, ISBN 978-960-474-076-5, p 91-95.
- [4] Diaconescu, D., *Products Conceptual Design* (Romanian), Transilvania University Publishing House, Brasov, 2005
- [5] Harvey, A., *Micro-hydro design manual*, TDG Publishing House, 2005.
- [6] Jaberg, H. Numerical methods for Fluid Dynamical Simulation of Hydro Power Plants. Proc. of 3rd WSEAS International Conference on Energy Planning, Energy Saving, Environmental Education, 3rd WSEAS RES 2009/3rd WSEAS WWAI 2009, pp. 399-413, July 1-3, 2009, Tenerife, Spain.
- [7] Jaliu, C., Diaconescu, D.V., Neagoe, M. and Săulescu R., *Dynamic features of speed increasers from mechatronic wind and hydro systems*, Proc. of EUCOMES 08, 2nd European Conf. on Mechanism Science, pp. 355-373, September 2008, Springer Publishing House, Cassino, Italy, 2008.
- [8] Jaliu, C., Diaconescu, D., Neagoe, M., Săulescu, R., Vătăşescu, M. *Conceptual synthesis of speed increasers for renewable energy systems*. The 10th IFToMM International Symposium on Science of Mechanisms and Machines, Braşov, SYROM 2009, September 12-15, pp. 171-183, 2009, ISBN: 978-90-481-3521-9, SpringerLink.
- [9] Jaliu, C., Săulescu, R., Diaconescu, D. and Neagoe, M. *Conceptual design of a chain speed increaser for small hydropower stations*. Proceedings of the ASME 2009 International Design Engineering Technical Conferences & Computers and Information in Engineering Conference, IDETC/CIE 2009, 30.08 – 2.09, 2009, San Diego, California, USA, CD Proceedings, ISBN: 987-0-7918-3856-3.
- [10] Neagoe, M. et al., *A Conceptual Design Application Based On A Generalized Algorithm*. The 19th International DAAAM Symposium. pp. 0953-0956, Trnava, Slovakia, 2008.
- [11] Neagoe, M., Diaconescu, D.V., Jaliu, C., Pascale, L., Săulescu, R. and Siscă, S., *On a New Cycloid Planetary Gear used to Fit Mechatronic Systems of RES*, OPTIM 2008. Proc. of the 11th Int. Conf. on Optimization of Electrical and Electronic Equipment. Vol. II-B. Renewable Energy Conversion and Control, pp. 439-449, Braşov, Romania, May 2008, IEEE Catalogue 08EX1996, 2008.
- [12] Sopian, K., Razak, JA. *Pico Hydro: clean power from small streams*, Proc. of 3rd WSEAS International Conference on Energy Planning, Energy Saving, Environmental Education, 3rd WSEAS RES 2009/3 WSEAS WWAI 2009, pp. 414-419, July 1-3, 2009, Tenerife, Spain.
- [13] Von Schon, H.A.E.C., *Hydro-Electric Practice - A Practical Manual of The Development of Water, Its Conversion To Electric Energy, And Its Distant Transmission*, France Press, 2007.